Soft Matter

RSC Publishing

PAPER

View Article Online
View Journal | View Issue

Cite this: *Soft Matter*, 2013, 9, 132

Fabrication of a shape memory hydrogel based on imidazole–zinc ion coordination for potential cell-encapsulating tubular scaffold application†

Wenjing Nan, Wei Wang, Han Gao and Wenguang Liu*

Received 17th August 2012
Accepted 26th September 2012

DOI: 10.1039/c2sm26918j

www.rsc.org/softmatter

A dipole–dipole reinforced copolymer hydrogel was synthesized by the one-step photopolymerization of vinylimidazole (VI) and acrylonitrile (AN) comonomer in the presence of a polyethylene glycol-based crosslinker. The mechanical properties of PVI–AN gels were tremendously increased by only chelating several mmol L^{-1} zinc ions, which was shown to firmly lock the temporary shape of the gel. Extraction of zinc ions by a complexing agent could facilitate the recovery of a permanent shape, and the memory behavior was reversible. The PVI–AN hydrogels supported the growth of L929 cells. The cell-seeded flat hydrogel sheet was folded into a temporary tubular scaffold and fixed in a culture medium containing 5 mmol L^{-1} zinc ions. After unfolding the tube, the exposed L929 cells were shown to adhere well on the surface of the gel. It is anticipated that this cell-loaded SM hydrogel could be fixed to a desired shape *in vitro* by small numbers of zinc ions for a potential implantable tissue engineering scaffold.

1 Introduction

Shape memory (SM) hydrogels represent a novel type of stimuli-responsive hydrogel that can memorize temporary shapes and revert to their permanent shape in response to external changes potentially including temperature, pH, electrical/magnetic field, light and ion strength.[1–15] However, several SM hydrogels reported to date are almost confined to the heat-activated transformation from a deformed state to the permanent shape.[1–6] Recently, our group observed for the first time a zinc ion-triggered triple shape memory effect in dipole–dipole reinforced ultra-high strength hydrogels. However, the dissociation of CN–CN dipole–dipole pairings occurred in merely 50% of zinc ions,[16,17] while such a high concentration of zinc ions is of no use in reality. Nonetheless, this Zn^{2+}-driven shape memory mechanism points out a new direction to design SM hydrogels. We can envisage if the hydrogel is mechanically strong enough to resist multi-form deformations, and along polymer chains there exist functional groups that can complex externally added metal ions, the introduced ion-crosslinkages would aid in stabilizing the temporary shape of the gel and then these ion crosslinkings are dissociated by a chelating agent, thus allowing the gel to resume its original form by which ion-induced shape memory can be achieved. It is well-documented that a variety of metal ions are able to strongly chelate amino and carboxyl groups at low concentrations.[18,19] A zinc finger is a small, functional, independently folded domain that coordinates one or more zinc ions to stabilize its structure through cysteine and/or histidine residues in which imidazole groups can bind strongly to zinc ions.[20] Inspired by this feature, we will synthesize a hydrogel based on an imidazole-containing monomer, acrylonitrile (AN) and a hydrophilic crosslinker in this study. It is anticipated that the strong dipole–dipole interaction in AN would enhance the strength of the hydrogel, and thus withstand the mechanical deformation. And AN–AN dipole–dipole pairings will not be destroyed in low concentration of zinc ions, which can dynamically complex and decomplex with imidazole moieties, thereby contributing to the reversible shape memory effect. We will also explore the ion-fixing shape memory hydrogel as a cell-carrying 3-D tube scaffold at low zinc ion concentration, expecting to extend its application in the biomedical field.

2 Experimental

2.1 Materials

1-Vinylimidazole (VI) was obtained from Aladdin Chemistry Corporation. Acrylonitrile (AN) was supplied by Kewei Company (Tianjin University, Tianjin China). Polyethylene glycol diacrylate (PEGDA, $M_n = 575$) and 2-hydroxy-4-(2-hydroxyethoxy)-2-methyl-propiophenone (IRGA-CURE-2959, 98%) were purchased from Sigma-Aldrich. 3-(4,5-Dimethyl-2-thiazoyl)-2,5-diphenyl tetrazolium bromide (MTT, 98%) was obtained from Alfa Aesar. All other chemicals were of analytical grade and were used without further purification.

School of Materials Science and Engineering, Tianjin Key Laboratory of Composite and Functional Materials, Tianjin University, Tianjin 30072, P. R. China. E-mail: wgliu@tju.edu.cn

† Electronic supplementary information (ESI) available. See DOI: 10.1039/c2sm26918j

2.2 Synthesis of P(VI-*co*-AN) hydrogels

P(VI-*co*-AN) hydrogels were synthesized by photoinitiated radical polymerization in DMSO using PEGDA as a cross-linker and IRGACURE-2959 as an initiator (3 wt%, relative to the total monomer mass). The initial monomer concentration in the feed was kept constant at 15 wt% and the weight ratio of total monomers, cross-linker and initiator was fixed at 2 : 1 : 0.09 for all the formulations. Different compositions of P(VI-*co*-AN) hydrogels were obtained by varying the VI : AN feed ratio (Table S1†). The reaction mixture was injected into plastic molds, and then the photo-polymerization was carried out for 30 min in a crosslink oven (XL-1000 UV Crosslinker, Spectronics Corporation, NY, USA). The resultant hydrogels were purified by immersing in distilled water, which was refreshed daily, for one week to remove the reagent residues completely. The obtained hydrogels were denoted as PVI–AN–X, where X represented the VI : AN weight ratio.

2.3 Characterization of P(VI-*co*-AN) hydrogels

Attenuated total reflection Fourier transform infrared spectroscopy (ATR-FTIR) spectra of dry hydrogels were recorded on a Perkin Elmer spectrum 100 (USA) to confirm the successful photopolymerization of hydrogels.

The equilibrium water contents (EWCs) of P(VI-*co*-AN) hydrogels were measured at room temperature. The gels were fully equilibrated in ultrapure water for at least 24 h, surface-dried with filter paper and then immediately weighed on a microbalance to measure the wet weight. Then these hydrogels were freeze-dried under a vacuum to achieve a constant weight. The EWC was defined as: $m_{eq} = (m_{wet} - m_{dry})/m_{wet} \times 100\%$, where m_{wet} and m_{dry} denote the wet weight and dry weight of the hydrogels, respectively. The average values of three measurements were taken for each sample.

The mechanical properties of hydrogels were measured on a WDW-05 electromechanical tester (Time Group Inc., China) at room temperature. Ultrapure water fully soaked hydrogels were cut into rectangular pieces with dimensions 20 mm × 2 mm × 0.3 mm for tensile strength tests. To minimize the effect of water evaporation, each experiment was performed over a short time period. Gauge length and crosshead speed were set as 10 mm and 100 mm min^{-1}, respectively. At least three specimens were tested for each sample.

2.4 Influence of zinc ions on the properties of hydrogels

The rectangular hydrogel strips with 20 mm × 2 mm × 0.3 mm dimensions were respectively immersed into different concentrations of $ZnSO_4$ and NaCl solutions. The stock solution of Zn^{2+} was prepared by dissolving $ZnSO_4 \cdot 7H_2O$ in distilled water. After reaching swelling equilibrium, the mechanical properties of the hydrogels were measured as described.

Distilled water-soaked hydrogel disc samples were separately immersed into different concentrations of Zn^{2+} and NaCl solutions. After two days, the diameter of each disc was measured in order to examine the influence of ions. In addition, the EWCs of each sample were also tested as mentioned above.

2.5 Evaluation of shape memory performance

The shape memory performance of the PVI–AN hydrogel was evaluated at room temperature. Hydrogels fully soaked in ultrapure water were cut into rectangular strips with dimensions 30 mm × 3 mm × 0.3 mm. The hydrogel pieces were curled into a spiral-like shape and put into an open-ended plastic tube to confine shape change. Subsequently, the plastic tube was placed in 1 mmol L^{-1} Zn^{2+} solution for 6 hours to fix the spiral shape. Then the spiral was taken out and dropped into 50 mmol L^{-1} EDTA solution at 37 °C to observe the recovery of the temporary shape.

Additionally, a serpentine glass tube was employed as the mold to acquire the original spring-shaped hydrogel sample. Afterwards, the fully equilibrated hydrogel was stretched and the two ends were fixed on a plastic plate. Shortly, the plastic plate was immersed in 10 mmol L^{-1} Zn^{2+} solution for 2 hours to fix the temporary shape of the gel. Then the stretched sample was peeled off and placed into 50 mmol L^{-1} EDTA solution at 37 °C to observe the recovery of the temporary shape.

2.6 Evaluation of shape memory cycle

The quantitative shape memory cycle was determined according to the reported method.[1] A straight strip of hydrogel was bent into a U-form shape and immersed into 1 mmol L^{-1} Zn^{2+} solution for 6 hours. Then the deformed hydrogel was transferred into 50 mmol L^{-1} EDTA solution at 37 °C to remove Zn^{2+} from the gel. The shape memory cycles were evaluated by measuring the angle at specific time points. The cycle was repeated three times. The shape fixity ratio (R_f) and shape recovery ratio (R_r) were defined by the following equation:[7]

$$R_f = \theta_t/\theta_i \times 100\%$$

$$R_r = (\theta_i - \theta_f)/\theta_i \times 100\%$$

where θ_i is the given angle, θ_t is the temporarily fixed angle and θ_f is the final angle.

2.7 Cytotoxicity assay of P(VI-*co*-AN) hydrogels

To evaluate the cytotoxicity of hydrogels, mouse fibroblasts (L929) were seeded in a 48-well plate coated with PVI–AN hydrogels and incubated for 48 h. Then the viability of the cells was determined by MTT assay for measurement of a viable cell number. The culture medium was replaced with 400 μL fresh medium containing 40 μL MTT (3-(4,5-dimethyl-2-thia-zoyl)-2,5-diphenyl tetrazolium bromide, 5 mg mL^{-1} in PBS), and the cells were incubated for another 4 h. Finally the whole medium was replaced by 300 μL DMSO per well to dissolve the formed crystal and the plate was gently shaken for 15 min. The absorbance of each well was measured at 490 nm on a Σ960 plate-reader (Metertech) with pure DMSO as a blank. The non-treated cell (in DMEM) was used as a control and the relative cell viability (mean% ± SD, $n = 3$) was expressed as $Abs_{sample}/Abs_{control} \times 100\%$.

The cytotoxicity of zinc ions against cells was examined in terms of the following procedure. The L929 cells were seeded in

a 48-well plate coated with hydrogels and incubated for 48 h. Subsequently, the culture medium was replaced with media containing different concentrations of zinc ions and the cells were incubated in the solution for 20 minutes. Then the cells were incubated for 48 h and the viability of the cells was determined by MTT assay.

2.8 Cells seeded into hydrogel tube fixed by zinc ions

L929 cells were seeded in a Petri dish coated with flat squares of PVI–AN hydrogel with dimensions 40 mm × 40 mm × 0.3 mm and incubated for 48 h at 37 °C in a 5% CO_2 humidified atmosphere. Then the cell-attached gel sheet was taken out and curled into a tubular-like shape. Immediately, the tubular-like gel was placed into a 5 mmol L^{-1} Zn^{2+} culture medium for 20 minutes to fix the tubular shape. After that, the gel was transferred to a culture medium containing 10% fetal bovine serum (FBS) and incubated for 2 h. Finally, the gel tube was unfolded to observe the cell attachment.

3 Results and discussion

3.1 Synthesis and characterization of hydrogels

The schematic molecular structure of the PVI–AN hydrogel is shown in Fig. 1A. The FTIR spectra of the copolymers (Fig. 1B) show that the bands at 1725 and 1083 cm^{-1} are separately attributed to the stretching vibrations of C=O and C–O in PEGDA. The feature peaks of vinylimidazole are located at 1645 cm^{-1}, which is a characteristic vibration of the imidazole ring.[21]

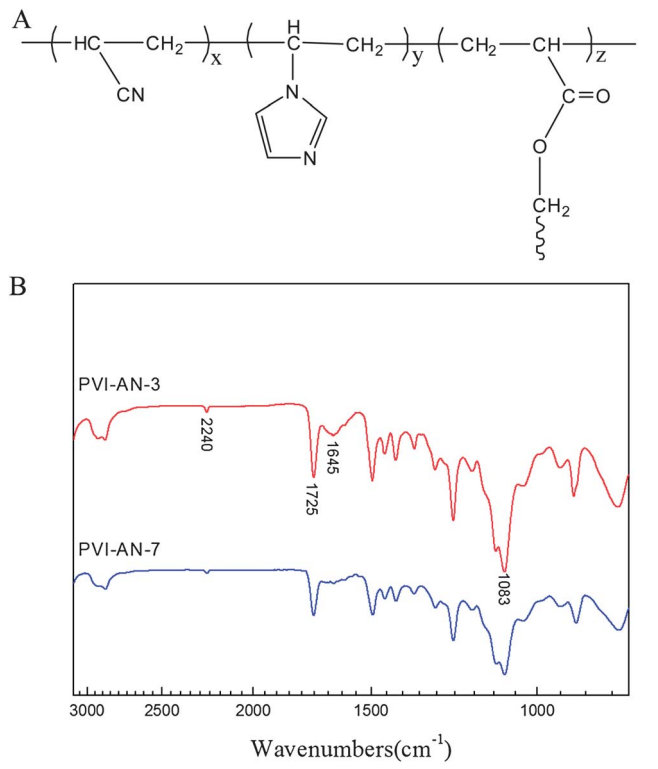

Fig. 1 Schematic molecular structure of PVI–AN hydrogel (A) and ATR-FTIR spectra of copolymers (B).

The band at 2240 cm^{-1} is attributed to the stretching vibration of C≡N.[22] These characteristic peaks suggest the formation of PVI–AN hydrogels.

The EWCs of PVI–AN hydrogels measured at room temperature are shown in Table S1.† In this study, only the effect of the VI : AN ratio on the EWC of the hydrogels was examined at a fixed initial monomer concentration and cross-linker content (Table S1†). One can see that the EWCs of the gels obtained a decrease from 87.1% to 67.5%, with an increase in AN content. It is obvious that introducing more CN–CN dipole–dipole interactions limits the water absorption of the gels. As shown in the table, the mechanical properties of hydrogels are positively correlated with the content of AN, evidencing the dipole–dipole reinforcement effect of AN.[23] Due to its appropriate EWC and mechanical properties, PVI–AN-3 will be chosen for the following shape memory evaluation.

3.2 Effect of zinc ions on the properties of hydrogels

The complexation of imidazole with transition metal ions is the foundation of the emerging shape memory effect in this study. To investigate the influence of the binding of zinc ions on the properties of gels, we immersed hydrogels into three different concentrations of Zn^{2+} solutions. For reference, the hydrogels were also fully soaked in the same three concentrations of NaCl solutions. After reaching swelling equilibrium, the properties of hydrogels were measured.

Fig. 2 exhibits tensile stress–strain force curves of PVI–AN hydrogels in different solutions. It is seen that the gels in Zn^{2+} solution show a significant improvement in their mechanical properties. However, hydrogels in the same concentrations of NaCl solutions display no noticeable change in strength. In the selected 1 mmol L^{-1}, 5 mmol L^{-1} and 10 mmol L^{-1} Zn^{2+} solutions, the tensile strengths of gels increase from 0.15 MPa in water to 0.88 MPa, 3.41 MPa and 4.00 MPa, respectively. Meantime, the Young's moduli are enhanced from 0.6 MPa in water to 8.11 MPa, 28.41 MPa and 37.84 MPa, respectively. These results indicate that the complexation of imidazole

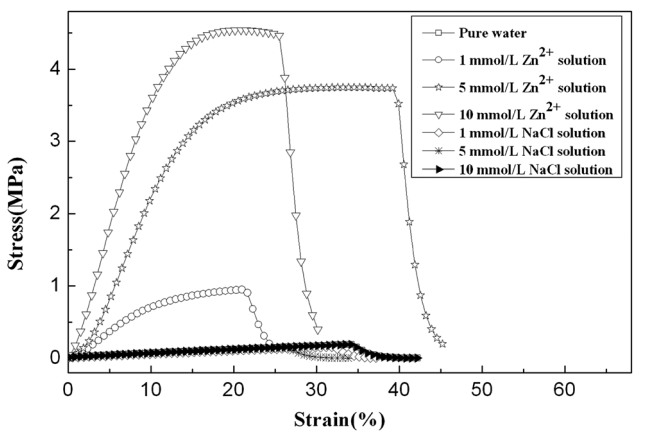

Fig. 2 Tensile stress–strain force curves of PVI–AN hydrogel under stretching in different concentrations of zinc ions and NaCl solutions. The NaCl solution serves as a control.

groups with Zn^{2+} acts as physical crosslinkage,[24,25] which leads to strong mechanical properties of hydrogels. From this perspective, the more linkages are formed with metal ions, the higher mechanical properties are achieved over a certain range. This effect can be demonstrated by comparing the strengths of hydrogels in the three concentrations of Zn^{2+} solution—at 5 mmol L^{-1} Zn^{2+}, a 22-fold increase in the tensile strength of the gel is observed. It is noted that the hydrogel could go back to its original mechanical strength determined in water while zinc ions were extracted from the gel by EDTA.

It is somewhat unexpected that the size of the hydrogel remains almost unchanged either in zinc ion or NaCl solution (Fig. S1A†). As for NaCl solution, the influence on swelling of the gels is driven by osmotic pressure. So the effect of osmotic pressure can be ignored at such low concentrations of ions. As aforementioned, the dramatic change in mechanical properties after immersing in zinc ion solution originates from the physical crosslinking between imidazole rings and zinc ions, while Fig. S1A† shows that the volume of gels does not shrink with the increase in crosslink points. We need to point out that there are two opposite variation trends in the volume of hydrogels upon immersing in Zn^{2+} solution. On the one hand, the attraction between zinc ions and imidazole rings may serve as crosslink points, which would lead to denser polymeric networks. On the other hand, zinc ion solution is weakly acidic due to its hydrolysis; in this case, the PVI network is prone to swelling because of protonation of imidazole moieties.[26] Analogously, the EWC of the hydrogel in 10 mmol L^{-1} zinc ion solution decreases only slightly, as shown in Fig. S1B.†

To quantify the amount of Zn^{2+} chelated by P(VI-*co*-AN) hydrogels, an atomic absorption spectroscopy assay was employed. Fig. S2† depicts the kinetics of Zn^{2+} adsorption onto P(VI-*co*-AN) hydrogel. The adsorption quantity shows a rapid increase with time and then reaches equilibrium within about 8 hours. The longer equilibrium adsorption time may result from the dense polymeric networks of the gels whose solid content is fixed at 15 wt% in this study. According to the equilibrium adsorption quantities of the zinc ion and the composition of the hydrogel, the average molar ratio of imidazole ring to the adsorbed zinc ions is roughly estimated to be about 14 : 1 in 1 mmol L^{-1} Zn^{2+} solution.

3.3 Shape memory performance

As depicted in Fig. 3, the original straight hydrogel strip was curled into tight spiral and could well be fixed in 1 mmol L^{-1} Zn^{2+} solution. Then the spiral was transferred into 50 mmol L^{-1} EDTA solution at 37 °C to remove zinc ions bound to the imidazole rings. The hydrogel lost its spiral shape rapidly, and it took less than 40 s to recover its permanent straight shape (Movie 1, ESI†). Based on the above analysis, a mechanism underlying a small amount of zinc ion-triggered reversible shape memory behavior can be portrayed in Fig. 4. While the deformed hydrogel is immersed into Zn^{2+} solution, the Zn^{2+}–imidazole coordination bonds formed act as additional crosslinking points, enhancing the elastic modulus and meanwhile firmly locking the temporary shape. Once the hydrogel is transferred into complexing agent solution, zinc ion–imidazole bonds are dissociated due to the extraction of zinc ions; consequently, the hydrogel is sharply decreased in modulus, and cannot prevent the gel from recovering to its permanent shape. It is noted that in pure water, although the deformed temporary shape of the gel could partially return to its original state owing to the diffusion of Zn^{2+} into water, this recovery process is very slow. Whereas adding complexing agent can remarkably facilitate the recovery kinetics.

We have demonstrated that PVI–AN hydrogels were able to recover their original straight strip shape from the temporary spiral shape after extracting zinc ions. Fig. S3† also clearly shows that PVI–AN gel can return to its original complicated spiral shape from the temporary strip shape after extracting zinc ions.

3.4 Shape memory cycle

In this study, shape fixity ratio (R_f) and shape recovery ratio (R_r) were used to evaluate the cyclicity of shape memory of PVI–AN hydrogels. All the R_f and R_r values of PVI–AN hydrogels at different VI : AN ratios reach 100% (Table S1†), indicating that imidazole–zinc ion binding can well lock the temporary shape and the decomplexation of this coordination can lead to full recovery of the original state. Fig. S4† displays the reproducible shape memory effects after three cycles.

3.5 Cytotoxicity assay and zinc ion-fixed hydrogel tube scaffold encapsulating cells

Cytotoxicity is one of the critical factors determining whether the hydrogel can be used in the biomedical field. Fig. 5A shows the phase contrast microscopy image of L929 cells on a

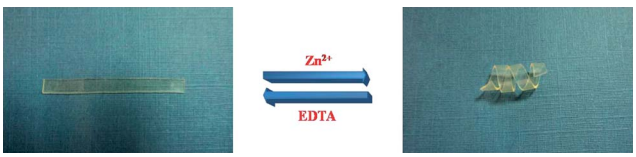

Fig. 3 Actual observation of the shape memory effect of PVI–AN hydrogel. The original straight hydrogel strip was curled into a tight spiral and fixed in 1 mmol L^{-1} Zn^{2+} solution. The spiral shape was transformed into the original strip shape after immersing in 50 mmol L^{-1} EDTA solution.

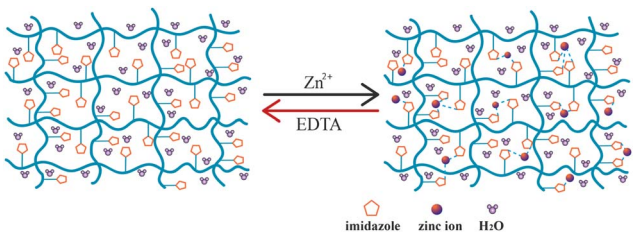

Fig. 4 A schematic diagram depicting the mechanism underlying a small number of zinc ions triggered reversible shape memory behavior. The imidazole rings coordinate with zinc ions; in EDTA solution, the Zn^{2+}–imidazole linkages are dissociated.

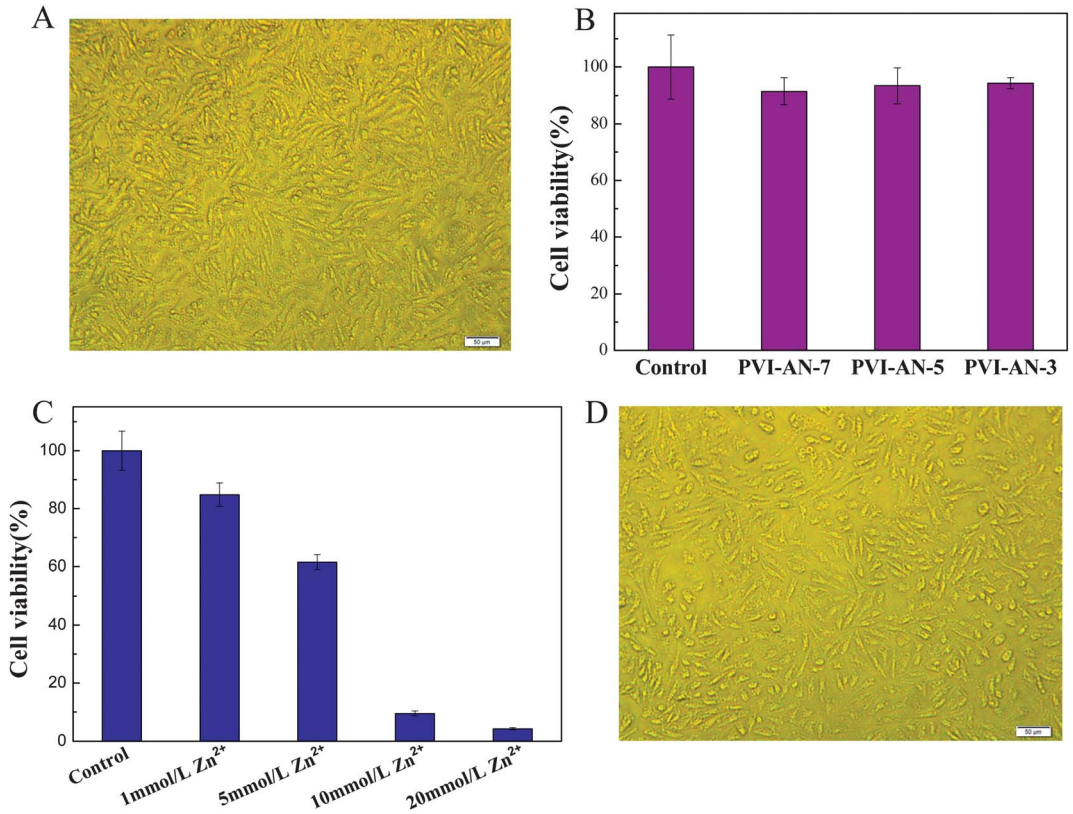

Fig. 5 (A) Phase contrast microscopy image of L929 cells cultured on PVI–AN gel at 37 °C. (B) Cell viability of L929 cells cultured on PVI–AN gel, as evaluated by the MTT assay. (C) Cell viability of L929 cells on PVI–AN gel fixed by different concentrations of zinc ions. (D) Phase contrast microscopy image of L929 cells adhered on the surface of the unfolded PVI–AN gel tube. Scale bars are 50 μm.

PVI–AN-3 hydrogel. The cells grow very well on the surface of the PVI–AN gel. Fig. 5B exhibits the viability of L929 cell lines examined on PVI–AN hydrogels with different VI : AN ratios. As shown in the figure, the PVI–AN gel can maintain about 90% cell viability at different monomer ratios, in comparison with non-treated cells used as a control.

The plain PVI–AN gel exhibits very good cytocompatibility, but the addition of zinc ions may cause the cytotoxicity.

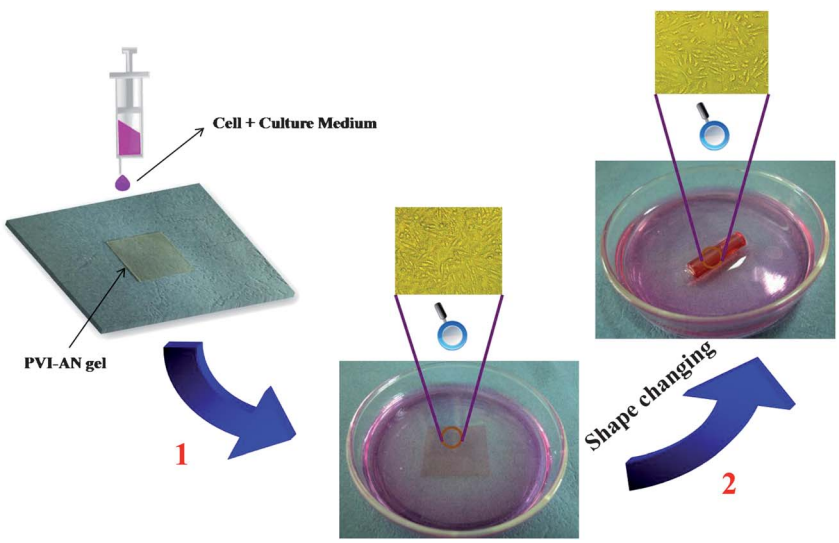

Fig. 6 Procedure depicting the formation of cell-encapsulating tubular hydrogel scaffold. (1) L929 cells were seeded on the flat square PVI-AN hydrogel; (2) the cell-attached gel sheet was taken out and curled into a tubular-like scaffold, which was immediately placed into 5 mmol L^{-1} Zn^{2+} culture medium for 20 minutes to fix the temporary shape.

Therefore, it is necessary to examine the toxicity of different concentrations of zinc ion solutions and thus select the concentration at which the temporary shape of the gel could be well fixed whilst retaining the viability of the cells. Fig. 5C shows the viability of L929 cell lines examined on PVI–AN hydrogels with different concentrations of zinc ions. The viability of the L929 cells drops dramatically with an increase in the concentration of zinc ions. Nonetheless, at 5 mmol L^{-1} zinc ion concentration, more than 60% of the cells remain viable. Taking into account the cytotoxicity of the zinc ion and the shape stability in the culture medium, 5 mmol L^{-1} zinc ion solution was used to fix the hydrogel tube. Fig. 6 shows that the square hydrogel sheet seeded with cells could be folded into a tube with cells on the inside. Then the tubular scaffold was fixed in the culture medium containing 5 mmol L^{-1} Zn^{2+} for 20 minutes. After that, the gel was transferred to the culture medium without zinc ions again, and incubated to inspect the stability of the tube shape and cell growth. We find that the tube could maintain its shape for 2 h, and L929 cells keep a normal morphology and adhere well on the surface of the unfolded hydrogel tube (Fig. 5D). This SM hydrogel may be potentially implanted *in vivo* as a tissue engineering scaffold after encapsulating seed cells and fixed to a desired shape *in vitro* by small amounts of zinc ions.

4 Conclusions

In summary, we have demonstrated that employing the complexation and decomplexation of imidazole groups with several mmol L^{-1} zinc ions can enable poly(1-vinylimidazole-*co*-acrylonitrile) hydrogels to memorize a temporary shape and recover to a permanent shape in a totally distinct way from traditional thermally induced SM hydrogels. This low cytotoxic shape memory hydrogel encapsulating cells can be fixed to a desired shape by small amounts of zinc ions *in vitro* and holds potential as a tissue engineering scaffold, thereby extending the application range of SM hydrogels.

Acknowledgements

The authors gratefully acknowledge the support for this work from the National Natural Science Foundation of China (Grants 50973082, 51173129, 21274105).

Notes and references

1 T. Hirai, H. Maruyama, T. Suzuki and S. Hayashi, *J. Appl. Polym. Sci.*, 1992, **45**, 1849–1855.
2 Y. Osada and A. Matsuda, *Nature*, 1995, **376**, 219.
3 T. Mitsumata, J. P. Gong and Y. Osada, *Polym. Adv. Technol.*, 2001, **12**, 136–150.
4 S. Chaterji, K. Kwon and K. Park, *Prog. Polym. Sci.*, 2007, **32**, 1083–1122.
5 P. J. Skrzeszewska, L. N. Jong, F. A. de Wolf, M. A. C. Stuart and J. van der Gucht, *Biomacromolecules*, 2011, **12**, 2285–2292.
6 K. Inomata, T. Terahama, R. Sekoguchi, T. Ito, H. Sugimoto and E. Nakanishi, *Polymer*, 2012, **53**, 3281–3286.
7 A. Lendlein and S. Kelch, *Angew. Chem., Int. Ed.*, 2002, **41**, 2035–2042.
8 E. Kurahashi, H. Sugimoto, E. Nakanishi, K. Nagata and K. Inomata, *Soft Matter*, 2012, **8**, 496–503.
9 I. Bellin, S. Kelch and A. Lendlein, *J. Mater. Chem.*, 2007, **17**, 2885–2891.
10 A. Lendlein, A. M. Schmidt and R. Langer, *Proc. Natl. Acad. Sci. U. S. A.*, 2001, **98**, 842–847.
11 P. Ping, W. S. Wang, X. S. Chen and X. B. Jing, *Biomacromolecules*, 2005, **6**, 587–592.
12 A. Lendlein, H. Y. Jiang, O. Junger and R. Langer, *Nature*, 2005, **434**, 879–882.
13 K. M. Lee, H. Koerner, R. A. Vaia, T. J. Bunninga and T. J. White, *Soft Matter*, 2011, **7**, 4318–4324.
14 Y. P. Cao, Y. Guan, J. Du, J. Luo, Y. X. Peng, C. W. Yip and A. S. C. Chan, *J. Mater. Chem.*, 2002, **12**, 2957–2960.
15 M. Bothe, K. Y. Mya, E. M. J. Lin, C. C. Yeo, X. H. Lu, C. H. He and T. Pretsch, *Soft Matter*, 2012, **8**, 965–966.
16 T. Bai, Y. J. Han, P. Zhang, W. Wang and W. G. Liu, *Soft Matter*, 2012, **8**, 6846–6852.
17 Y. J. Han, T. Bai, Y. Liu, X. Y. Zhai and W. G. Liu, *Macromol. Rapid Commun.*, 2012, **33**, 225–231.
18 J. F. Shi, Y. Gao, Y. Zhang, Y. Pan and B. Xu, *Langmuir*, 2011, **27**, 14425–14431.
19 B. Hai, J. Wu, X. F. Chen, J. D. Protasiewicz and D. A. Scherson, *Langmuir*, 2005, **21**, 3104–3105.
20 S. V. Razin, V. V. Borunova, O. G. Maksimenko and O. L. Kantidze, *Biochemistry*, 2012, **77**, 217–226.
21 L. Bromberg, L. Chen, E. P. Chang, S. Wang and T. A. Hatton, *Chem. Mater.*, 2010, **22**, 5383–5391.
22 L. F. Zhang and Y. L. Hsieh, *Nanotechnology*, 2006, **17**, 4416–4423.
23 T. Bai, P. Zhang, Y. J. Han, Y. Liu, W. G. Liu, X. L. Zhao and W. Lu, *Soft Matter*, 2011, **7**, 2825–2831.
24 B. Sharma, J. S. Rao and G. N. Sastry, *J. Phys. Chem. A*, 2011, **115**, 1971–1984.
25 S. Sjoberg, *Pure Appl. Chem.*, 1997, **69**, 1549.
26 A. Horta, M. J. Molina, M. R. Gomez-Anton and I. F. Pierola, *Macromolecules*, 2009, **42**, 1285–1287.